SUPPLEMENTARY MATERIALS
FOR

Enabling adoption of 2D-NMR for the higher order structure assessment of monoclonal antibody therapeutics

Robert G. Brinson[a,*], John P. Marino[a], Frank Delaglio[a], Luke W. Arbogast[a], Ryan M. Evans[b], Anthony Kearsley[b], Geneviève Gingras[c], Houman Ghasriani[c], Yves Aubin[c], Gregory K. Pierens[d], Xinying Jia[d], Mehdi Mobli[d], Hamish G. Grant[e], David W. Keizer[e], Kristian Schweimer[f], Jonas Ståhle[g], Göran Widmalm[g], Edward R. Zartler[h], Chad W. Lawrence[i], Patrick N. Reardon[i,†], John R. Cort[i], Ping Xu[j], Feng Ni[j], Saeko Yanaka[k], Koichi Kato[k], Stuart R. Parnham[l], Desiree Tsao[m], Andreas Blomgren[n], Torgny Rundlöf[n], Nils Trieloff[o], Peter Schmieder[o], Alfred Ross[p], Ken Skidmore[q], Kang Chen[r], David Keire[r], Darón I. Freedberg[s], Thea Suter-Stahel[t], Gerhard Wider[t], Gregor Ilc[u,v], Janez Plavec[u,v], Scott A. Bradley[ww], Donna M. Baldisseri[x], Mauricio Luis Sforça[y], Ana Carolina de Mattos Zeri[z] Julie Yu Wei[aa], Christina M. Szabo[bb], Carlos A. Amezcua[bb], John B. Jordan[cc], Mats Wikström[dd]

[a]Institute of Bioscience and Biotechnology Research, National Institute of Standards and Technology and the University of Maryland, Rockville, MD, USA; [b]Applied and Computational Mathematics Division, National Institute of Standards and Technology, Gaithersburg, MD, USA; [c]Centre for Biologics Evaluation, Biologics and Genetic Therapies Directorate, Health Canada, Ottawa, ON, Canada; [d]The Centre for Advanced Imaging, The University of Queensland, St Lucia QLD, Australia; [e]Bio21 Molecular Science & Biotechnology Institute, The University of Melbourne, Victoria, Australia; [f]Lehrstuhl Biopolymere, Universitaet Bayreuth, Bayreuth, Germany; [g]Department of Organic Chemistry, Arrhenius Laboratory, Stockholm University, Stockholm, Sweden; [h]Analytical R&D, Pfizer Essential Health, Lake Forest, IL, USA; [i]Pacific Northwest National Laboratory, Earth and Biological Sciences Directorate, Richland, WA, USA; [j]Department of Downstream Processing and Analytics, Human Health Therapeutics Research Centre, National Research Council of Canada, Montreal, Quebec, Canada; [k]Institute for Molecular Science and Exploratory Research Center on Life and Living Systems, National Institutes of Natural Sciences, Myodaiji, Okazaki, Japan; [l]Department of Biochemistry and Molecular Biology, Medical University of South Carolina, Charleston, SC, USA; [m]Analytical Development, Momenta Pharmaceuticals, Cambridge, MA, USA; [n]Laboratory Unit, Swedish Medical Products Agency, Uppsala, Sweden; [o]NMR-supported Structural Biology, Leibniz-Forschungsinstitut für Molekulare Pharmakologie (FMP), Berlin, Germany; [p]Roche Pharmaceutical Research & Early Development, Pre-Clinical CMC, Roche Innovation Center Basel, F. Hoffmann-La Roche Ltd, Basel, Switzerland; [q]Analytical Operations, Genentech, South San Francisco, CA, USA; [r]Center for Drug Evaluation and Research, Food and Drug Administration, Silver Spring, MD, USA; [s]Center for Biologics Evaluation and Research, Food and Drug Administration, Silver Spring, MD, USA; [t]Department of Biology, Institute of Molecular Biology and Biophysics, ETH Zurich, Zurich, Switzerland; [u]NMR Centre, EN-FIST Centre of Excellence, Ljubljana, Slovenia; [v]NMR Centre, National Institute of Chemistry, Ljubljana, Slovenia; [w]Eli Lilly and Company, Lilly Corporate Center, Indianapolis, IN, USA; [x]MRS – Application Science, Bruker BioSpin Corporation, Billerica, MA, USA; [y]Brazilian Biosciences Laboratory (LNBio), Brazilian Center for Research in Energy and Materials (CNPEM), Campinas, Brazil; [z]Brazilian Synchrotron Light Laboratory (LNLS), Brazilian Center for Research in Energy and Materials (CNPEM), Campinas, Brazil; [aa]Protein Product Development, Biogen Inc., Cambridge, MA, USA; [bb]Baxter Pharmaceuticals R&D, Baxter Healthcare, Round Lake, IL, USA; [cc]Global Regulatory and R&D Policy, Amgen Inc., Thousand Oaks, CA, USA; [dd]Higher Order Structure, Attribute Sciences, Amgen Inc., Thousand Oaks, CA, USA

*Contact: e-mail, robert.brinson@nist.gov, 240-314-6336
[†]Present address: Oregon State University, Corvallis, Oregon 97331, United States

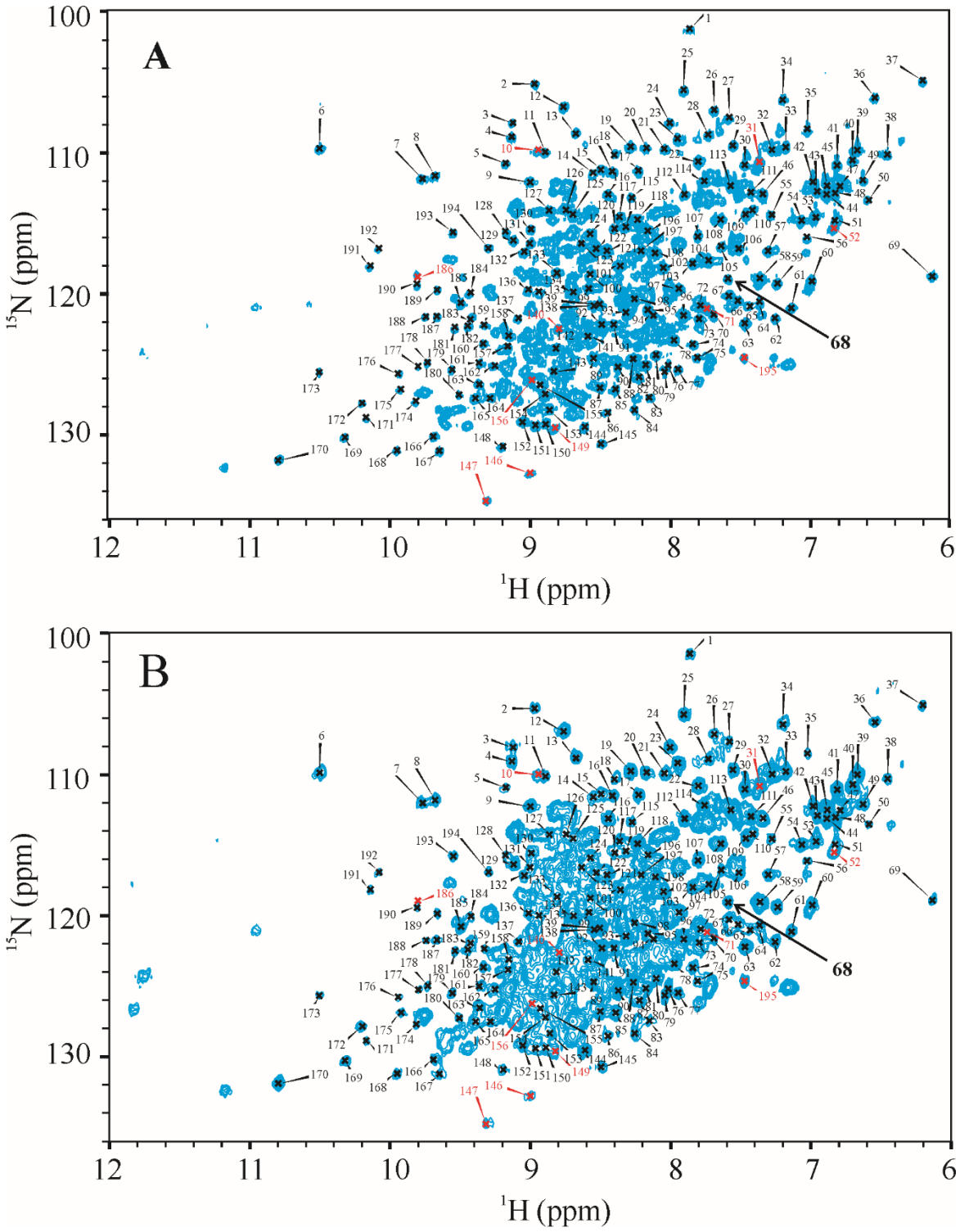

Figure S1. Representative ^{1}H,^{15}N gHSQC spectral fingerprints for the SSS at 900 MHz and 500 MHz showing the peaks with arbitrary numbering used for CCSD precision analyses. (**A**) D1A-8495-009 spectrum at 900 MHz; (**B**) D1A-9966-001 spectrum at 500 MHz. Both representative spectra were collected at 37 °C. Contour levels were chosen for best visualization of the picked peaks. The arbitrarily numbered peak lists were initially defined from a 500 MHz gHSQC spectrum for the SSS and copied to all other spectra. All ^{1}H,^{15}N spectra were aligned to

arbitrary cross peak #68 (see arrow). The peaks in red were subsequently removed from the list due to poor resolution or S/N in a subset of spectra. Arbitrary cross peaks 146 and 147 were removed due to a subset of spectra recorded with reduced ^{15}N spectral width, leading to folding of these two cross peaks (experimental code: E2). Due to the relatively few number of spectra measured on the NIST-Fab, no attempt was made to define a common peak list between the NIST-Fab and SSS. For spectra of SSS collected at different temperatures, many cross peaks shifted significantly due to the temperature difference, resulting in peak tracking error. As a result, only $^{1}H,^{15}N$ spectra collected at 37 °C were included in the peak list tables. See Materials and Methods section for more details.

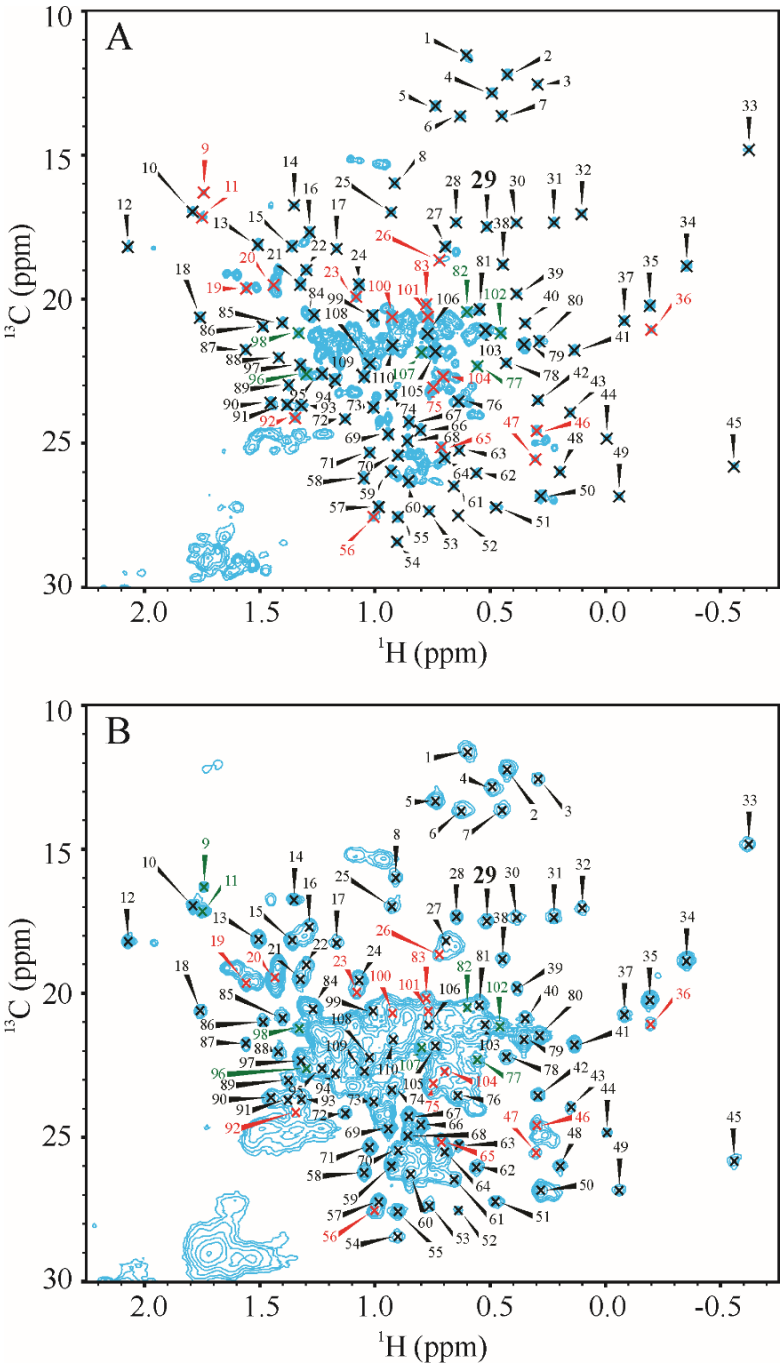

Figure S2. Representative ^{1}H,^{13}C gHSQC spectral fingerprints for the SSS at 900 MHz and 500 MHz showing the peaks with arbitrary numbering used in CCSD and chemometric analyses. (**A**) D2C-8495-012 spectrum at 900 MHz; (**B**) D2C-3897-012 spectrum at 500 MHz. Both representative spectra were collected at 37 °C. Contour levels were chosen for best visualization of the picked peaks. A common arbitrarily numbered peak list was initially defined from a 500 MHz gHSQC spectrum for both the SSS and NIST-Fab at 37 °C and copied to all other ^{1}H,^{13}C spectra at all temperatures. All ^{1}H,^{13}C spectra were aligned to arbitrary cross peak #29, shown in bold. The peaks in red were subsequently removed from the list due to poor resolution or S/N in a subset of spectra. The peaks in green were not resolved in the SOFAST-HMQC spectra (spectral code: E2C). See Materials and Methods section for more details.

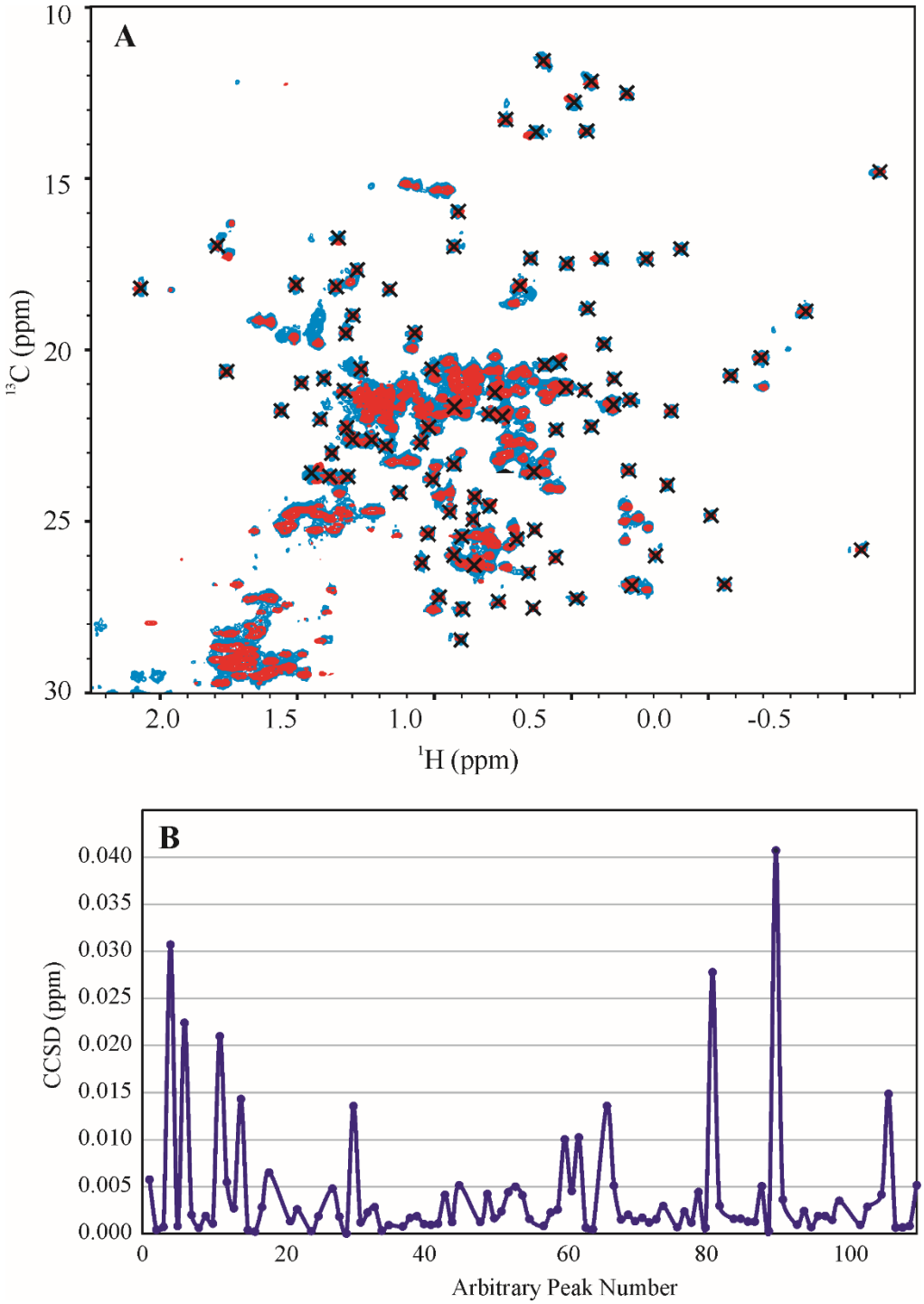

Figure S3. Comparative analysis of the common peak list. (**A**) Overlays of D2C-7425-012 of SSS and D3A-7425-015 of the NIST-Fab representative ^{1}H,^{13}C gHSQC spectral fingerprints at 900 MHz with the common peak list from **Figure S2**. These common peaks are marked with an 'X.' For clarity, all excluded peaks not used for further analysis are removed from this overlay (see **Figure S2** caption for more details.) (B) CCSD plot of D3A-7425-015 spectrum of the NIST-Fab at 900 MHz benchmarked against the average uniformly sampled D2A/D2C reference peak positions. As can be seen in **Figures 2E, F** and **S3**, the ^{1}H,^{13}C spectrum contained additional peaks

due to the four extra amino acids on the N-termini of both the heavy and light chains of the SSS. However, since these extra cross peaks were not common to both samples, they were not used in the analyses. The differences between the SSS and NIST-Fab spectra highlighted by PCA can therefore be explained by the shifting of a number of resonances by up to 40 ppb.

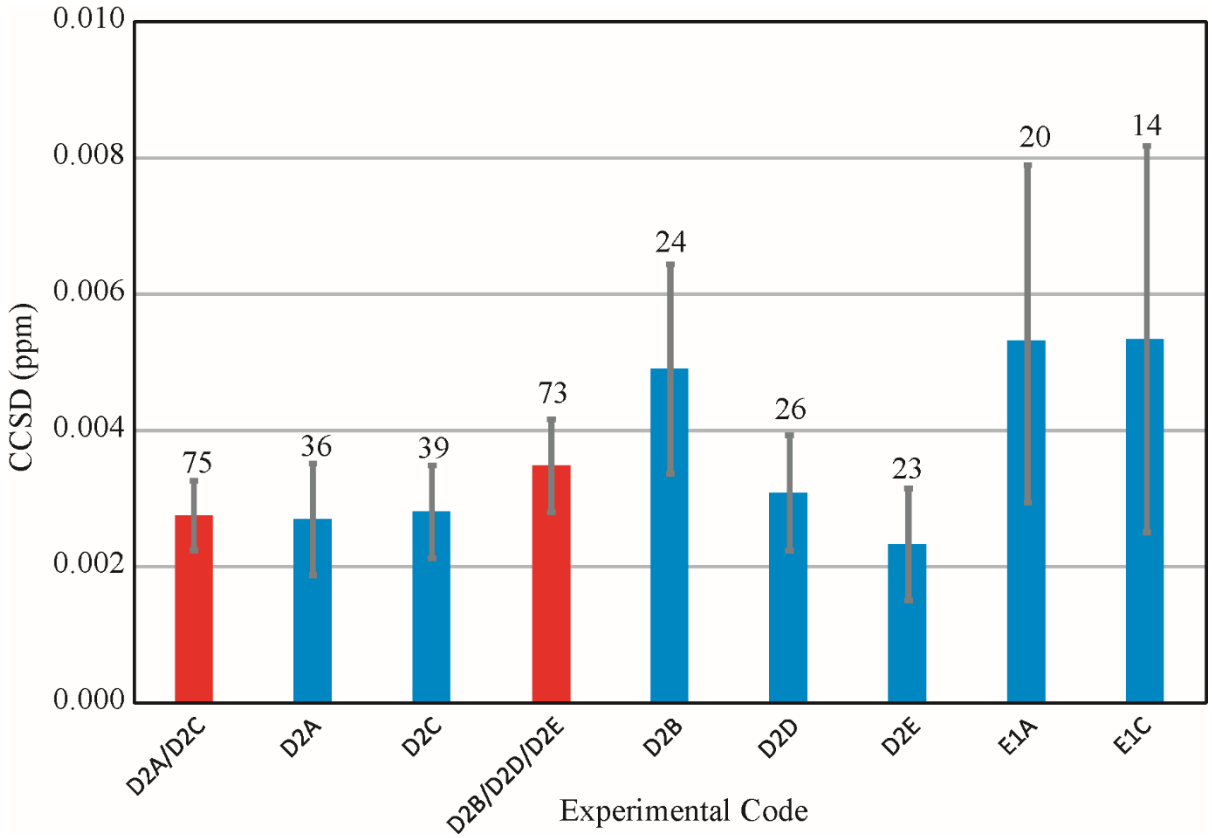

Figure S4. Breakdown of $^{1}H,^{13}C$ CCSD analysis of the SSS recorded at 37 °C. In general, all spectra were collected with a gHSQC, with the exception of E1C spectra, which used the SOFAST-HMQC pulse sequence. The red bars represent average CCSD values for D2A/D2C US spectra and D2B/D2D/D2E NUS spectra, respectively. The bolded number above each bar represents the total number of spectra included in the analysis for each respective experimental type. Custom NUS E1A-type experiments tended to have slightly less peak precision, highlighting the need for careful selection of NUS schedule. Error bars represent 95% confidence intervals for standard error of the mean (SEM). For detailed breakdown of experimental codes, see **Table 1** in the main text.

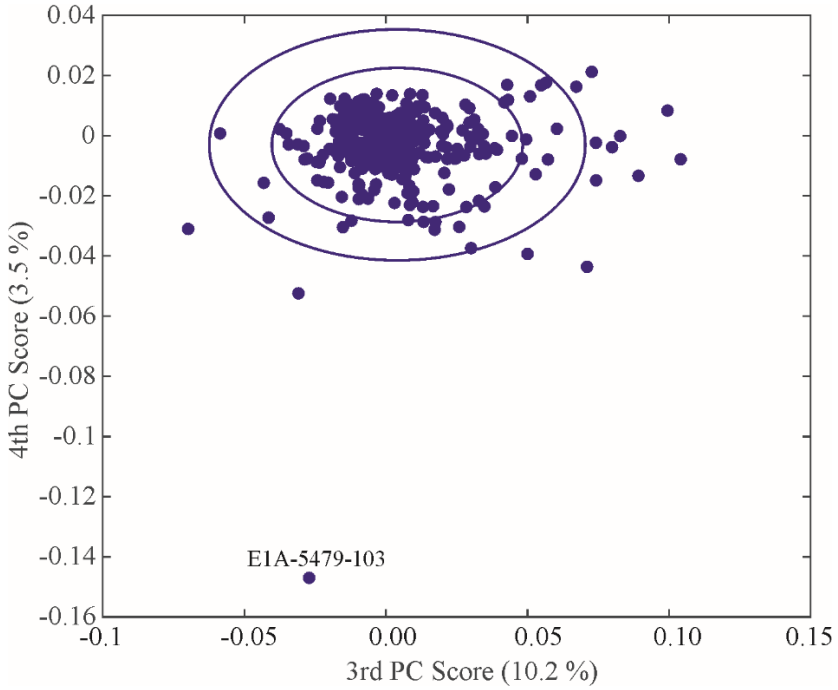

Figure S5. Highlight of PC4 outlier from PCA of all peak lists from 354 $^{1}H,^{13}C$ spectra. The only substantial PC4 outlier, spectrum E1A-5479-103, is labeled. The inner and outer ellipsoids represent 95% and 99% confidence regions, respectively, based on chi-square probabilities. See the caption of **Figure S6** for more details.

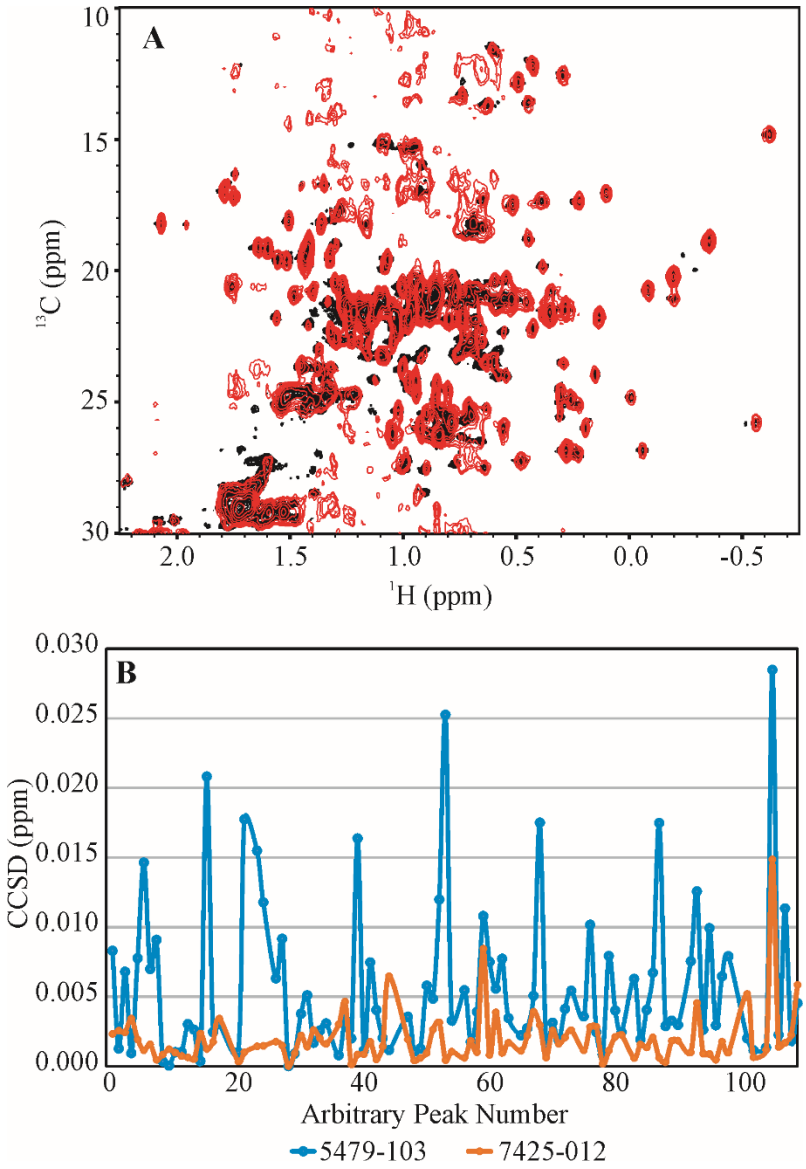

Figure S6. Analysis of a representative outlier ^{1}H,^{13}C spectrum E1A-5479-103. (**A**) Overlay of E1A-5479-103 NUS spectrum recorded at 500 MHz in red, with uniform sampled D2C-7425-012 spectrum collected at 900 MHz in black. (**B**) CCSD plot of E1A-5479-103 versus D2C-7425-012, both benchmarked against the average uniformly sampled D2A/D2C reference peak positions. E1A-5479-103 was collected with a custom NUS schedule that was generated with the manufacturer's software, TopSpin 3. Unlike the NIST NUS schedules that were generated with the Poisson-gap algorithm, the custom NUS schedule for 5479-103 contained many holes at the beginning of the schedule, leading to the observed artifacts. As can be seen in the CCSD plot in panel **B**, a subset of resonances were also shifted from the average uniformly sampled D2A/D2C reference peak positions. However, despite these shifts, the majority of resonances still were under 10 ppb from the reference. The effect of sampling schedule is beyond the scope of this manuscript.

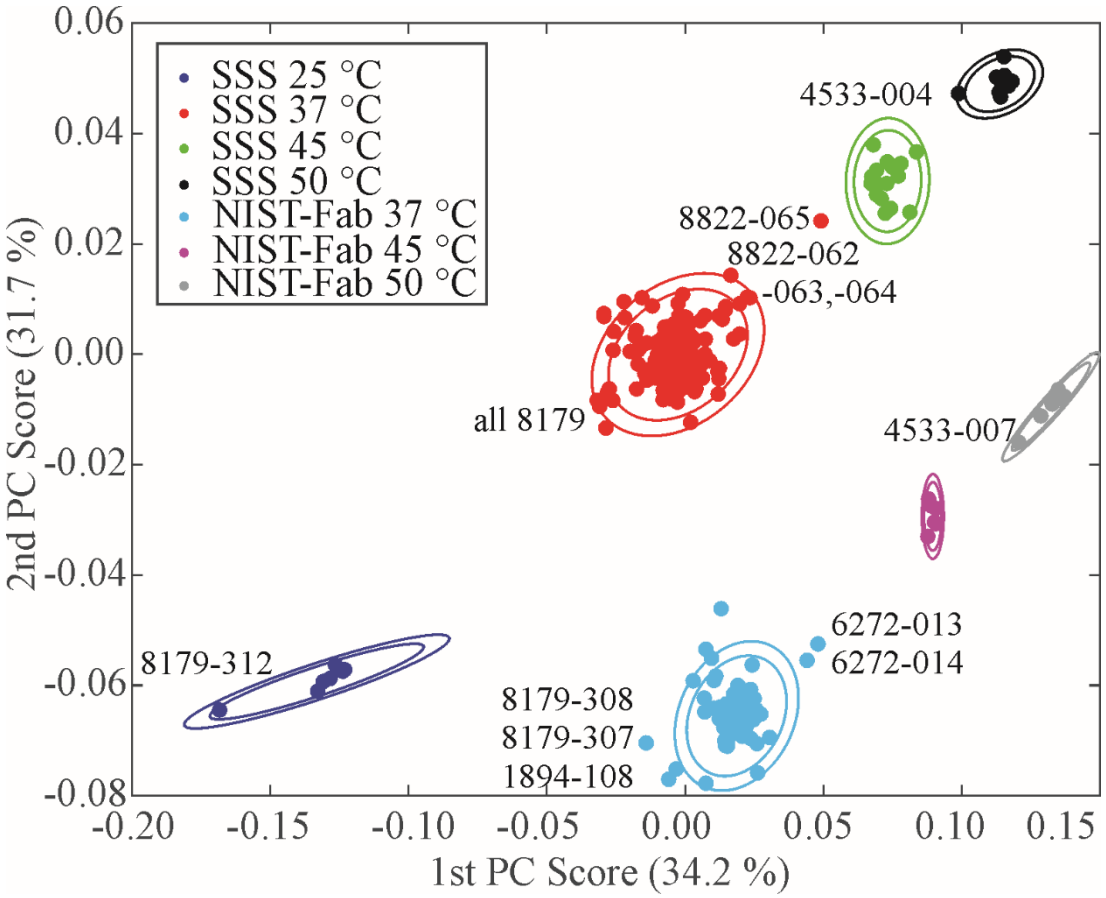

Figure S7. Annotated PCA plot of temperature deviant outlier $^{1}H,^{13}C$ spectra from **Figure 4A** of the main text. Several SSS spectra were determined to be deviant from the reported temperature. For the NIST-Fab outlier spectra labeled on the plot, these are likely temperature deviant as well due to the high spectral similarity of the NIST-Fab to the SSS even though no calibration curve was made. The inner and outer ellipsoids represent 95% and 99% confidence regions, respectively, based on chi-square probabilities. **Figure S8** shows a representative example of a $^{1}H,^{13}C$ spectrum with shifted peaks due to temperature, and **Table S2** lists the calculated temperatures from calibration curves using selected $^{1}H,^{13}C$ chemical shift positions.

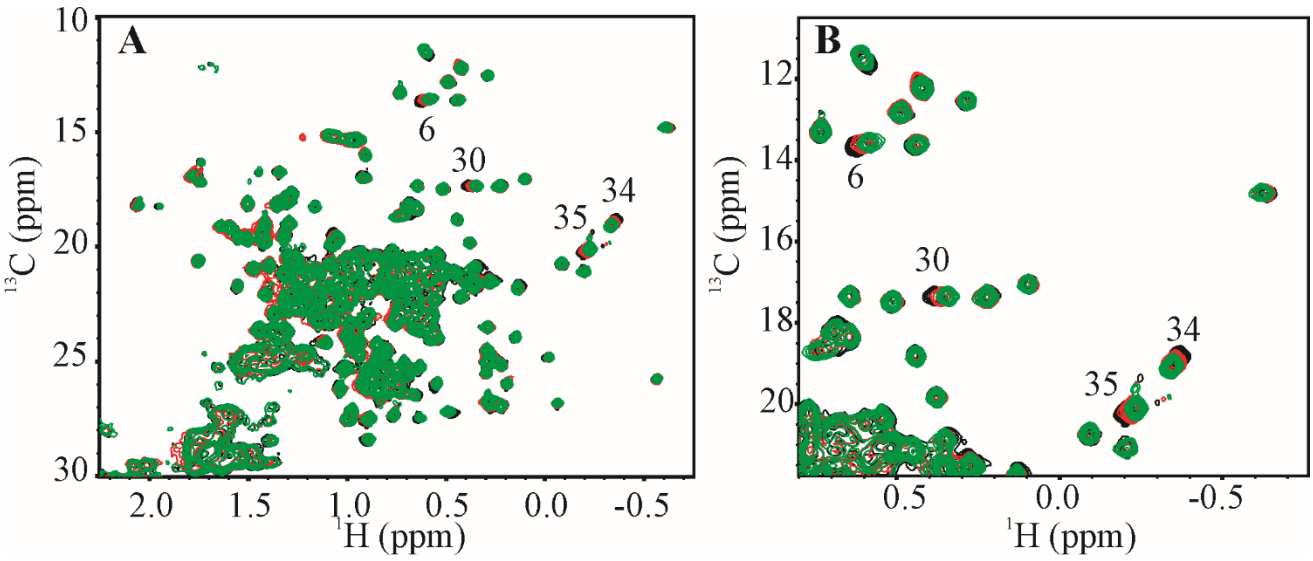

Figure S8. Overlay of SSS temperature outlier at 600 MHz. The outlier ^{1}H,^{13}C gHSQC spectrum of D2E-8822-065 is in red, D2C-8822-036 at 37 °C in black, and E1B-8822-051 at 45 °C in green. (**A**) Complete methyl fingerprint region; (**B**) Expansion showing the four cross peaks that exhibited temperature sensitivity. Relevant temperature-sensitive arbitrarily-numbered cross peaks used to generate temperature calibration curves are labeled. Laboratory 8822 recorded these spectra on two different 600 MHz spectrometers.

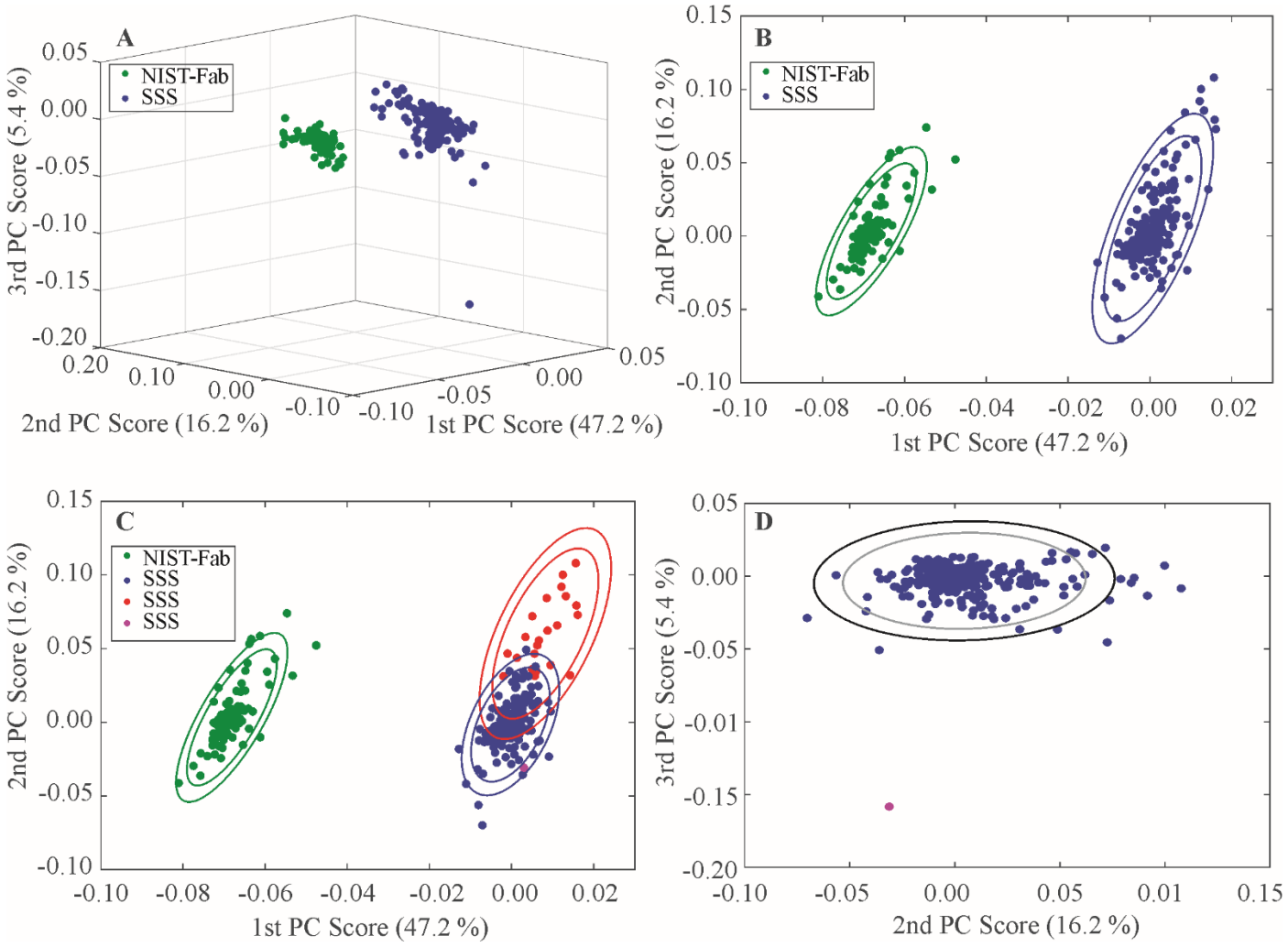

Figure S9. *k*-Medoids clustered PCA plots of peak tables from $^{1}H,^{13}C$ spectra recorded at 37 °C. All peak tables were clustered with the *k*-medoids clustering algorithm. (**A**) 3D plot of two clusters ($k = 2$); (**B**) 2D plot of the same two clusters ($k = 2$) clusters; (**C**) 2D plot of four clusters ($k = 4$). (**D**) 2D plot of PC2 versus PC3. To simplify panel **D**, all clusters ($k = 4$) were colored the same with the exception of the PC3 outlier in magenta. The magenta point in panels **C** and **D** is spectrum E1A-5479-103, which the *k*-medoids algorithm clustered as its own individual group and outside all confidence intervals. The inner and outer ellipsoids represent 95% and 99% confidence regions, respectively, based on chi-square probabilities. For more discussion of panels **B** and **C**, see **Figure S10**, for which the data is annotated differently to highlight the likely relevant differences between $k = 2$ and $k = 4$ clusters. See **Figure S6** for more discussion of this outlier.

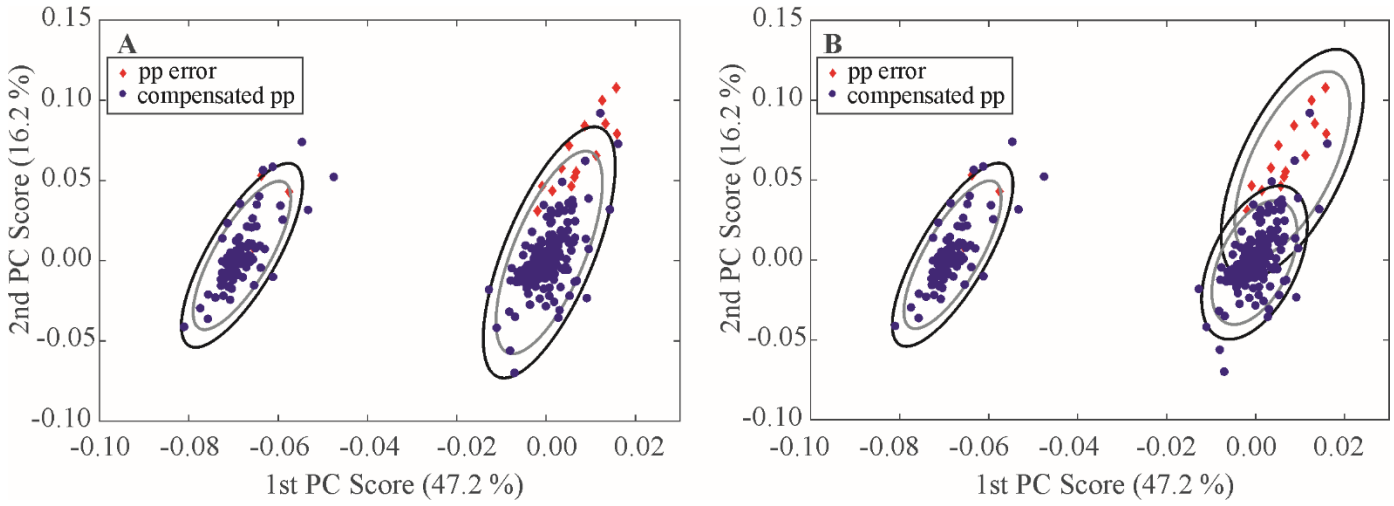

Figure S10. Re-annotated *k*-medoids clustered PCA plots of peak tables from $^{1}H,^{13}C$ spectra recorded at 37 °C. As in **Figure S9**, all peak tables were clustered with the *k*-medoids clustering algorithm. (**A**) Two clusters (k = 2); (**B**) Four clusters (k = 4). The inner and outer ellipsoids represent 95% and 99% confidence regions, respectively, based on chi-square probabilities. For both panels, red diamonds represent a subset of spectra collected with a known pulse program (pp) error. The pulse program error arose on some NUS spectra that were recorded on Bruker spectrometers that used the software TopSpin 2. On this version of TopSpin, NUS acquisition needed to be hard-coded into the pulse program, whereas TopSpin 3, used on all other Bruker spectrometers, allowed facile implementation of NUS within the software. For the TopSpin 2 version of the pulse sequence, an uncompensated ^{15}N decoupling pulse was present during ^{13}C evolution, resulting in spectra that could not be appropriately phased in the ^{13}C dimension. In panel **B** this subset of NUS spectra collected on TopSpin 2 pulse sequence error appears to have been loosely clustered by the *k*-medoids clustering algorithm. The spectra with this systematic error are denoted in the center column of **Table S10**.

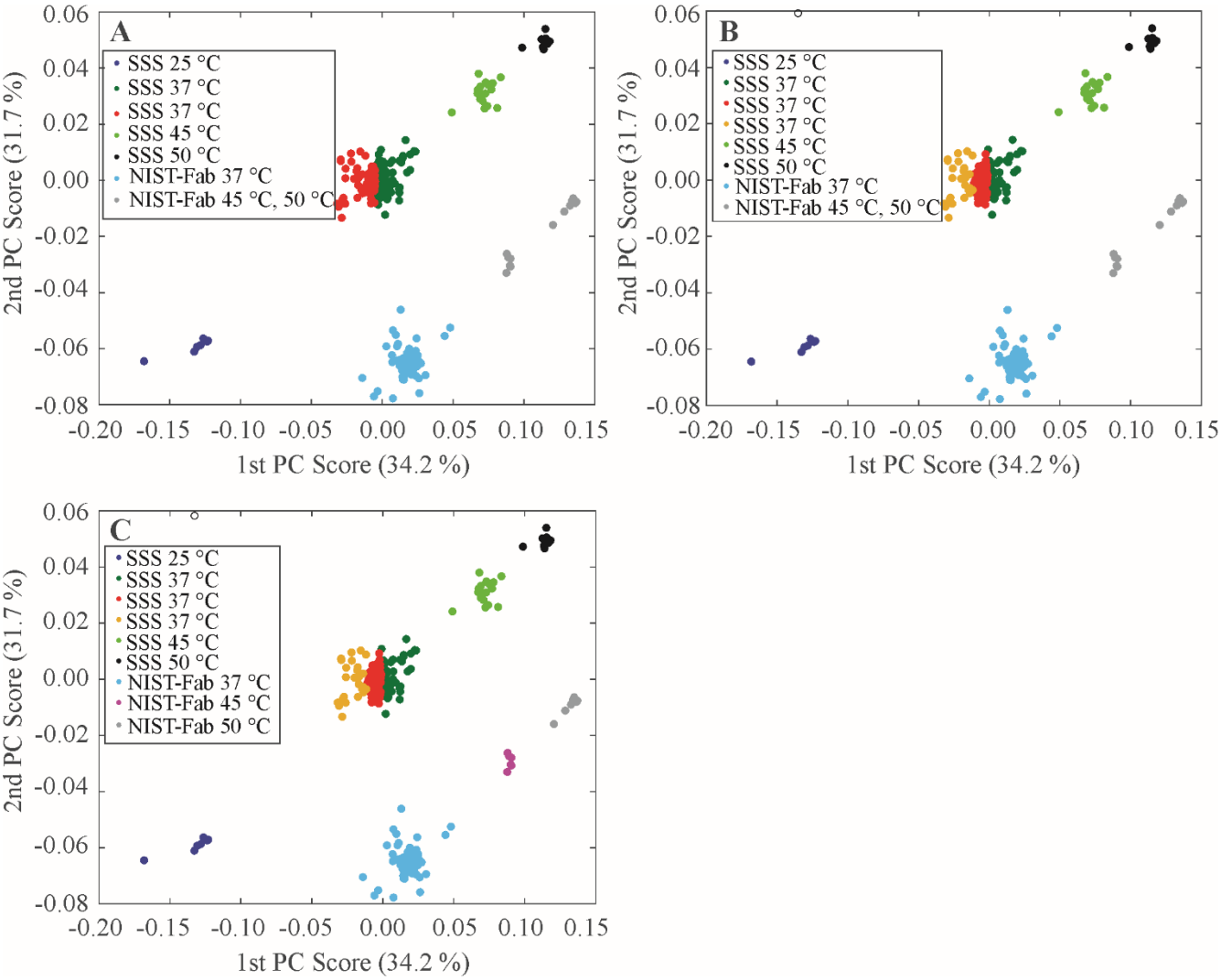

Figure S11. Data clustered with the *k*-medoids algorithm using two principal components (PCs). (**A**) $k = 7$; (**B**) $k = 8$; (**C**) $k = 9$. The clustering results clearly show that the *k*-medoids algorithm is less effective at analyzing this data set, since it divides the 37 °C SSS spectra into two or three distinct clusters. Furthermore, the *k*-medoids algorithm groups the NIST-Fab spectra ($k = 7$ and 8) collected at 45 °C with the NIST-Fab spectra collected at 50 °C. When 9 clusters were explicitly specified, the algorithm divided these two sets of spectra separate into their appropriate clusters.

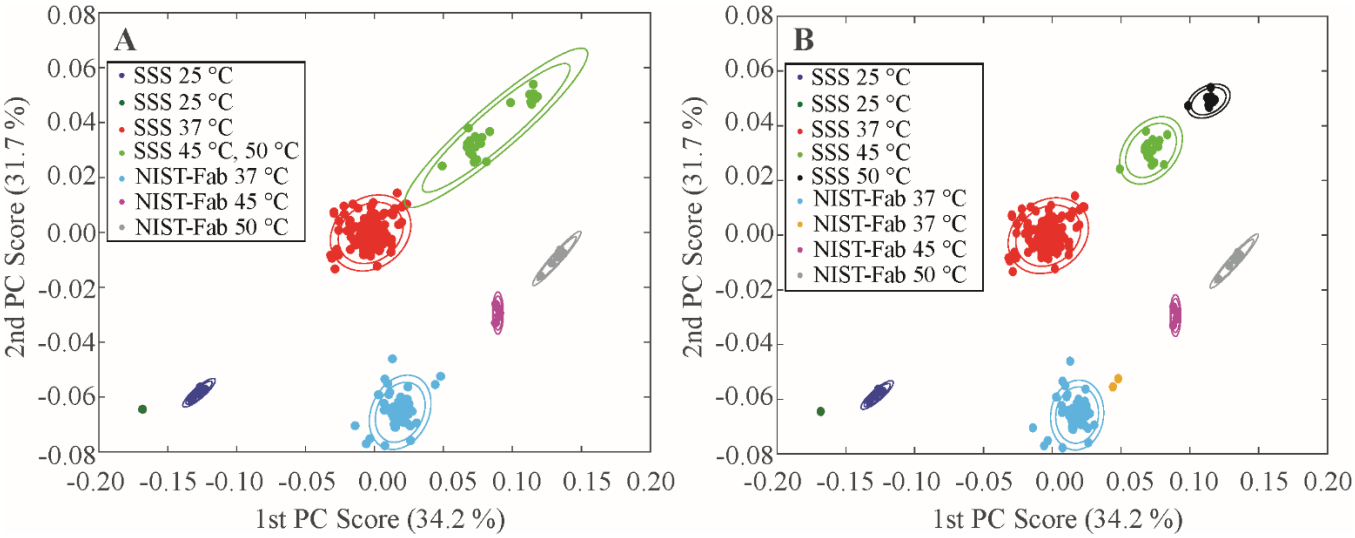

Figure S12. Data clustered using the min-max group pair algorithm using two principal components. (**A**) k = 7; (**B**) k = 9. The inner and outer ellipses depict 95% and 99% confidence regions, respectively, based on chi-square probabilities. For panel **A**, it is seen that this algorithm detected an outlier and placed this spectrum in its own cluster. This singleton cluster (dark green) represents a single spectrum E1B-8179-312 that is a known temperature outlier (**Table S2**). Additionally, the placement of spectrum E1B-8179-312 in its own cluster had the effect of grouping the SSS spectra collected at 45 °C with the SSS spectra collected at 50 °C. For k = 8, the incorrect temperature cluster was appropriately separated out into distinct groups (**Figure 4B**, main text). In panel **B**, two known NIST-Fab spectral outliers, D3A-6272-013 and D3B-6272-014, due to temperature are separated into a distinct cluster (in orange). It should be noted that UPGMA produces identical clusters to the min-max group pair algorithm when k = 8 and k = 9.

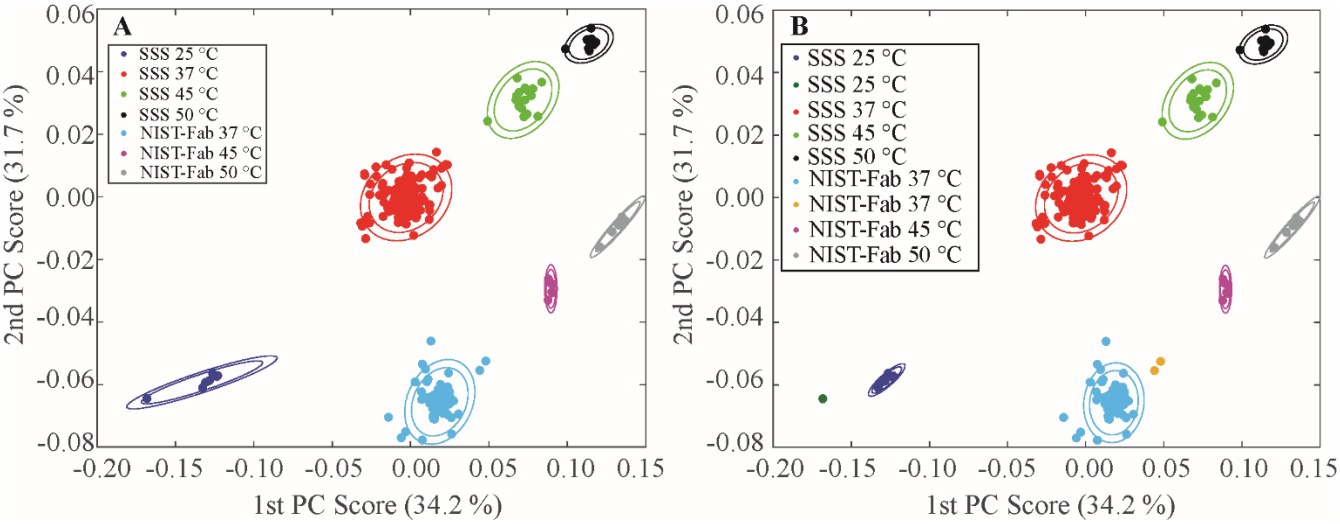

Figure S13. Data clustered using the UPGMA algorithm using two principal components (**A**) k = 7; (**B**) k = 9. The inner and outer ellipses depict 95% and 99% confidence regions, respectively, based on chi-square probabilities. For panel **A**, it is seen that this algorithm correctly clustered the spectra, including the addition of D2E-8822-065 into the SSS 45 °C cluster. For k = 8, spectrum E1B-8179-312 is then separated out into its own singleton cluster (**Figure 4B**, dark green point, **Table S2**). In panel **B**, two known NIST-Fab spectral outliers, D3A-6272-013 and D3B-6272-014, due to temperature are separated into a distinct cluster (in orange). It should be noted that UPGMA produces identical clusters to the min-max group pair algorithm when k=8 and k=9.

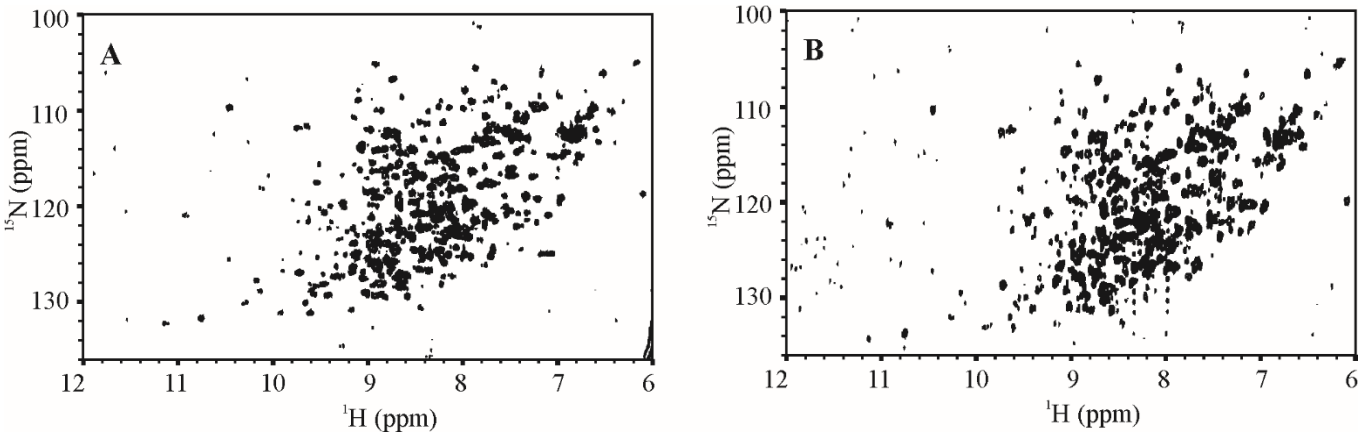

Figure S14. Representative ^{1}H, ^{15}N gHSQC spectral fingerprint outliers not included in the peak analysis. (**A**) D1A-7244-014 spectrum of SSS at 800 MHz; (**B**) E2-3655-101 of SSS at 800 MHz. All representative spectra were collected at 37 °C. Many cross peaks in these two representative spectra are missing or have very low S/N. Compare to **Figure 1** in the main text. All excluded spectra are listed in **Table S10**. These excluded spectra suggest the need for care in experimental set-up rather than a problem with 2D-NMR method. Unfortunately, they also represent a weakness in peak analysis. If a spectral perturbation occurs in the fingerprint region that does not impact one of the defined peaks, such a perturbation would be missed. A total point-by-point analysis of the entire spectral region will 'catch' any such spectral change, although this type of analysis is also sensitive to field strength, pulse sequence, and sampling schedule. A total point-by-point analysis could also help evaluate the severity of possible experimental errors and how these may adversely affect the analysis of the spectral fingerprint.

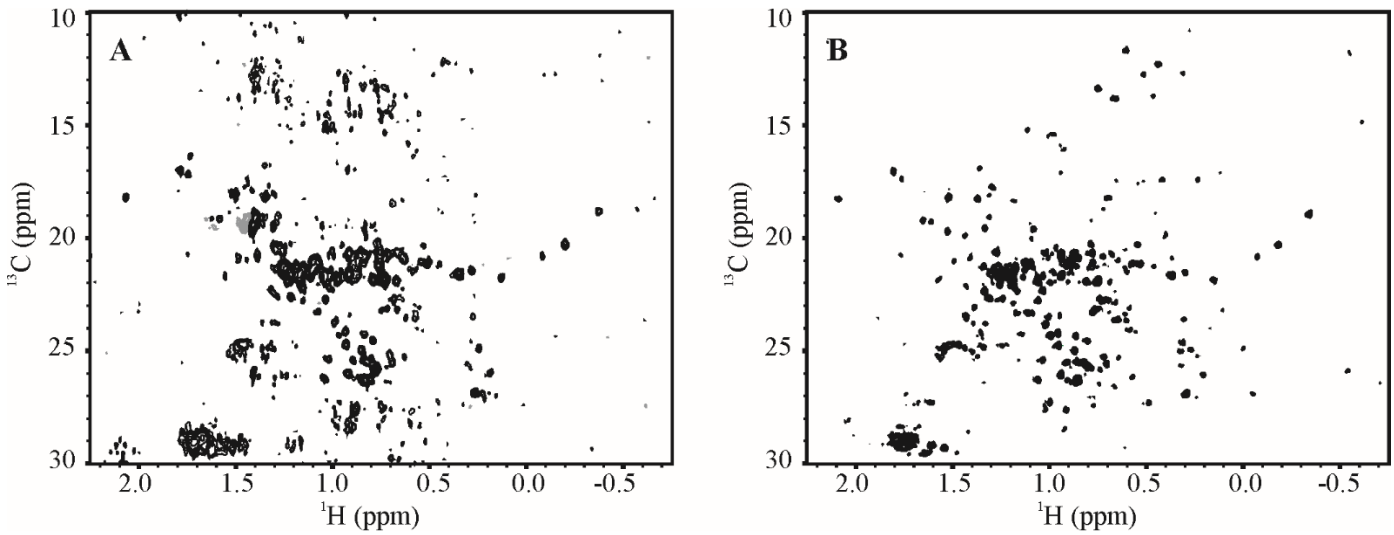

Figure S15. Representative ^{1}H, ^{13}C gHSQC spectral fingerprint outliers not included in the peak analysis. (**A**) E1A-1894-103 spectrum of SSS at 600 MHz; (**B**) D3B-2461-107 of the NIST-Fab at 800 MHz. All representative spectra were collected at 37 °C. Positive contours are in black and negative contours in gray. Both spectra are plotted just above the noise threshold. Many cross peaks in these two representative spectra are missing or have very low S/N. In addition, the arbitrarily numbered cross peak used for alignment (peak #29, see **Figure S2**) is missing or has extremely weak intensity, precluding accurate spectral alignment. Compare to **Figure 2** in the main text. All excluded spectra are listed in **Table S10**. See Materials and Methods in main text and **Figure S14** caption for more details.

Table S1. Detailed summary of the experiments performed by each institution. Institutions who submitted more than one data package received multiple institutional identifiers. See **Table 1** in main text for the description of each experimental code.

Institutional Identifier	Total by Institution	D1A	D2A	D2B	D2C	D2D	D2E	D3A	D3B	E1	E1A	E1B	E1C	E2	E2N	E2A	E2B	E2C
1247	**12**	1	1	0	1	0	0	0	0	2	5	0	2	0	0	0	0	0
1894	**8**	0	1	0	1	0	0	1	0	0	4	0	0	1	0	0	0	0
2146	**8**	1	1	1	1	1	1	1	1	0	0	0	0	0	0	0	0	0
2461	**8**	1	1	1	1	1	0	1	1	0	0	0	0	0	0	0	1	0
2974	**8**	1	1	1	1	1	1	1	1	0	0	0	0	0	0	0	0	0
3655	**4**	0	0	0	1	0	0	1	0	0	0	0	0	2	0	0	0	0
3676	**6**	0	1	0	1	0	0	0	0	1	1	0	0	2	0	0	0	0
3897	**24**	3	3	3	3	3	3	3	3	0	0	0	0	0	0	0	0	0
4233	**88**	2	3	2	3	2	2	4	4	0	15	32	12	0	0	4	0	3
4533	**3**	0	0	0	0	0	0	0	0	0	0	2	0	0	0	0	1	0
5417	**20**	2	2	2	2	2	2	4	4	0	0	0	0	0	0	0	0	0
5422	**8**	1	1	1	1	1	1	1	1	0	0	0	0	0	0	0	0	0
5479	**10**	0	1	0	1	1	1	2	2	0	1	0	0	1	0	0	0	0
5487	**8**	1	1	1	1	1	1	1	1	0	0	0	0	0	0	0	0	0
6211	**12**	0	1	4	1	1	1	1	1	0	1	0	0	1	0	0	0	0
6272	**21**	0	3	2	3	3	1	2	2	0	0	0	0	3	0	0	1	1
6324	**23**	1	2	1	2	1	1	2	0	0	5	3	0	0	1	3	1	0
7244	**16**	2	2	2	3	2	1	2	2	0	0	0	0	0	0	0	0	0
7425	**16**	2	2	2	2	2	2	2	2	0	0	0	0	0	0	0	0	0
8179	**13**	1	1	0	1	0	0	1	0	0	5	1	0	0	0	1	1	1
8473	**8**	0	1	1	1	1	1	1	1	0	0	0	0	1	0	0	0	0
8495	**21**	2	2	2	2	2	2	2	3	4	0	0	0	0	0	0	0	0
8543	**9**	1	1	0	1	0	0	1	0	0	5	0	0	0	0	0	0	0
8822	**65**	4	3	3	3	3	3	9	4	0	0	10	7	0	1	6	3	6
9516	**8**	1	1	1	1	1	1	1	1	0	0	0	0	0	0	0	0	0
9936	**10**	1	1	1	1	1	1	1	1	0	0	0	2	0	0	0	0	0
9963	**7**	1	1	1	1	1	0	1	1	0	0	0	0	0	0	0	0	0
9966	**7**	1	1	0	1	0	0	1	0	0	3	0	0	0	0	0	0	0

Table S2. Corrected temperatures for outlier $^{1}H,^{13}C$ spectra of SSS in the PCA plot. Temperature calibration curves were separately generated for ^{1}H and ^{13}C resonance positions for arbitrarily numbered cross peaks, 6, 30, 34, and 35 and averaged. For peak 30, only the ^{1}H chemical shift was used due to negligible perturbation of the ^{13}C chemical shift. See **Figure S8**.

Experimental Type‡	Experimental Code	Field (MHz)	Reported Temperature	Corrected Temperature
D2A	8822-061	600	37 °C	39.1 °C
D2B	8822-062	600	37 °C	39.6 °C
D2C	8822-063	600	37 °C	39.5 °C
D2D	8822-064	600	37 °C	39.0 °C
D2E	8822-065	600	37 °C	42.9 °C
D2A	8179-302	500	37 °C	35.0 °C
E1A	8179-303	500	37 °C	34.6 °C
D2C	8179-304	500	37 °C	34.6 °C
E1A	8179-305	500	37 °C	34.6 °C
E1A	8179-306	500	37 °C	35.4 °C
E1B	8179-312	500	25 °C	22.7 °C
E1B	4533-004	600	50 °C	48.3 °C

‡See **Table 1** in main text for complete description of experimental types.

Table S3. Percent of resolved $^{1}H,^{13}C$ methyl cross peaks for the unlabeled NIST-Fab sample at 37 °C. The SSS data were not used in this analysis. This analysis of the NIST-Fab spectra was performed on the D3A-type experiments with 25 ms acquisition time in the ^{13}C dimension. A total of 232 cross peaks were expected to be observed from 25 alanines, 11 isoleucines (2 cross peaks each), 32 leucines (2 cross peaks each), 5 methionines, 44 threonines, and 36 valines (2 cross peaks each). Lower percent coverage is observed at 500 MHz for the common peak list between the NIST-Fab and the SSS (**Table S12**) because this list covers all acquisition strategies and temperatures explored in this study. Using a peak table for a single molecule (*e.g.*, the NIST-Fab) with a single field strength and experimental set-up affords much higher spectral coverage even at 500 MHz.

Field (MHz)	Number of Picked Peaks	% Coverage
900	212	91
850	209	90
800	207	89
750	201	87
700	194	85
600	180	78
500	155	67

Table S4. Complete instrument list. The institutional identifier and equipment list were anonymized by NAPT to further reduce potential data traceability. Rows in blue, QCI cold probes; row in gray, BBO cold probe; rows in white, TCI or other cold probe; rows in orange, room temperature probe; rows in green, Agilent/Varian equipment.

^{1}H Frequency	Vendor	Console	Probe
500 MHz	Bruker BioSpin	Avance III	CP QCI H/F-C/C-D CryoProbe, Z-gradients
500 MHz	Bruker BioSpin	Avance II+	5mm TCI 1H-13C/15N/D CryoProbe, Z-gradients
500 MHz	Bruker BioSpin	Avance III-HD	CP BBO 500S2 BBF-H-D-05 Z-gradients
600 MHz	Agilent/Varian	INOVA	5mm Triple Resonance (1H,13C,15N,2H) cold probe, Z-gradients
600 MHz	Agilent/Varian	DD2	Triple resonance PFG cold probe
600 MHz	Bruker BioSpin	Avance III HD	5mm TCI 1H-13C/15N/D CryoProbe, Z-gradients
600 MHz	Bruker BioSpin	Avance III HD	5mm TCI 1H-13C/15N/D CryoProbe, Z-gradients
600 MHz	Bruker BioSpin	Avance III	PA BBO 600S3 BBB-H-D-05 Z SP
600 MHz	Bruker BioSpin	Avance III	CP QCI 600S3 H/F-C/N-D-05 Z-gradients
600 MHz	Bruker (Oxford)	Avance II+	5mm QCI 1H-13C/15N/31P/D CryoProbe, Z-gradients
600 MHz	Bruker BioSpin	Avance III HD	5 mm CP TCI 1H/19F-13C/15N/D Z-gradients
600 MHz	Bruker BioSpin	Avance III	5mm DCH 1H/13C/D CryoProbe, Z-gradients
600 MHz	Bruker BioSpin	Avance III	5mm TXI 1H-13C/15N/D triple-resonance probe, Z-gradients
600 MHz	Bruker BioSpin	Avance III	5mm TCI 1H-13C/15N/D CryoProbe, Z-gradients
600 MHz	Bruker BioSpin	Avance III	5mm TCI 1H-13C/15N/D CryoProbe, Z-gradients
600 MHz	Bruker BioSpin	Avance	Cold, 13C/15N/31P tunable 1H/19F
600 MHz	Bruker BioSpin	Avance III HD	CP TCI 600S3 H&F-C/N-D-05 Z-gradients
600 MHz	Bruker BioSpin	Avance III	5mm TCI 1H-13C/15N/D CryoProbe, Z-gradients
600 MHz	Bruker BioSpin	Avance	5mm TXI 1H-13C/15N/D RT probe, z-gradients

700 MHz	Bruker BioSpin	Avance III	5mm TCI 1H-13C/15N/D CryoProbe, Z-gradients
700 MHz	Bruker BioSpin	Avance III	5mm TCI 1H-13C/15N/D CryoProbe, Z-gradients
700 MHz	Bruker BioSpin	Avance III	5mm TCI CryoProbe, xyz-gradients
700 MHz	Bruker BioSpin	Avance III HD	5mm H{C/N} Cryo (13C enhanced), Z-gradients
700 MHz	Bruker BioSpin	Avance III	5mm TCI 1H-13C/15N/D CryoProbe, Z-gradients
700 MHz	Bruker BioSpin	Avance III	5mm TCI 1H-13C/15N/D CryoProbe, Z-gradients
750 MHz	Bruker BioSpin	Avance III	5mm TXI 1H-13C/15N/D RT probe, Z-gradients
750 MHz	Bruker BioSpin	Avance III	5mm TCI 1H-13C/15N/D CryoProbe, Z-gradients
800 MHz	Agilent/Varian	VNMRS	5mm ColdProbe gen 2, 1H-13C/15N/D, Z-gradients
800 MHz	Agilent/Varian	VNMRS	Triple resonance PFG cold probe
800 MHz	Bruker BioSpin	Avance III	5mm TCI 1H-13C/15N/D CryoProbe, Z-gradients
800 MHz	Bruker BioSpin	Avance III	5mm TCI 1H-13C/15N/D CryoProbe, Z-gradients
800 MHz	Bruker BioSpin	Avance III	5mm TXI 1H-13C/15N/D probe, Z-gradients
800 MHz	Bruker BioSpin	Avance III HD	5mm TCI CryoProbe
850 MHz	Bruker BioSpin	Avance III	5mm TCI 1H-13C/15N/D CryoProbe, Z-gradients
850 MHz	Bruker BioSpin	Avance III	TCI, Z-gradients
850 MHz	Bruker BioSpin	Avance III	5mm QCI 1H-13C/15N/31P/D CryoProbe, Z-gradients
900 MHz	Bruker BioSpin	Avance III HD	5mm TCI 1H-13C/15N/D CryoProbe, Z-gradients
900 MHz	Bruker (Oxford)	Avance III HD	5mm TCI CryoProbe
900 MHz	Bruker BioSpin	Avance III	5mm TCI 1H-13C/15N/D CryoProbe, Z-gradients

Table S5. Experimental parameters for the required D1A experiment: $^{1}H,^{15}N$ gHSQC

Scans per Increment	Enough scans per increment collected to achieve an average minimum S/N of 10:1
Recycling Delay	*Discretion of individual laboratory; typically 1.0 s – 1.5 s*
J^{1}_{NH}	93 Hz
^{1}H Carrier Position	Water resonance
^{1}H Sweep Width	20 ppm
^{1}H Acquisition time	100 ms
^{15}N Carrier Position	117 ppm
^{15}N Sweep Width	40 ppm
^{15}N Acquisition Time	20 ms (See **Table S6** for number of total points)
Sampling Schedule	Uniform
Temperature	37 ± 0.1 °C

Table S6. Varied experimental parameters for the required D1A experiment: $^{1}H,^{15}N$ gHSQC

Field (MHz)	^{15}N Acquisition Time	^{15}N Total Points
500	20 ms	82
600	20 ms	98
700	20 ms	114
750	20 ms	122
800	20 ms	132
850	20 ms	138
900	20 ms	146

Table S7. Experimental parameters for the required ^{1}H,^{13}C gHSQC experiments. The overall goal was to achieve an average S/N of at least 10:1.

Scans per increment	**System Suitability Ssample** **Experiments D2A - D2D**: Same number of scans per increment **Experiment D2E**: Twice the scans per increment of Experiment D2C **Unlabeled NIST-Fab** **Experiment D3A:** Scans per increment set to achieve S/N of at least 10:1 **Experiment D3B:** Same number of scans per increment as Exp. D3A
Recycling Delay	*Discretion of individual laboratory; typically 1.0 s – 1.5 s*
J^{1}_{CH}	145 Hz
^{1}H Carrier Position	Water resonance
^{1}H Sweep Width	14 ppm
^{1}H Acquisition time	100 ms
^{13}C Carrier Position	20 ppm
^{13}C Sweep Width	30 ppm
^{13}C Acquisition Time	Varied, see **Table S8**
Temperature	37 ± 0.1 °C

Table S8. Varied experimental parameters for the required $^{1}H,^{13}C$ gHSQC experiments

	Experiments D2A, D2B		Exp. D2C, D2D, D2E, D3A, D3B	
Field (MHz)	**^{13}C Acquisition Time**	**^{13}C Total Points‡**	**^{13}C Acquisition Time**	**^{13}C Total Points‡**
500	17.0 ms	128	25 ms	188
600	14.1 ms	128	25 ms	226
700	12.1 ms	128	25 ms	264
750	11.3 ms	128	25 ms	282
800	10.6 ms	128	25 ms	302
850	10.0 ms	128	25 ms	320
900	9.4 ms	128	25 ms	338

‡For NUS experiments, sampling schedule was 50%.

Table S9. Recommended parameters for the optional SOFAST-HMQC E1C- and E2C-type experiments. Some laboratories performed these experiments with different shape pulses.

	$^{1}H,^{15}N$ Experiment	**$^{1}H,^{13}C$ Experiment**
Acquisition time, t_2	50 ms	50 ms
Excitation Pulse	Pc.9.90	Pc.9.90
Refocusing Pulse	Reburp	Reburp
Excitation Window	5.55 ppm	4.44 ppm
Center of Shape Pulses	8.25 ppm	0.0 ppm

Table S10. Spectra excluded from peak analysis due to poor S/N or poor resolution. An average S/N of at least 10:1 was required for each peak list. For the spectra with the known pulse program error (see **Figure S10**), these were not included in the CCSD analysis (center column) but were included in the PCA plots. In addition, only peak lists of the SSS recorded at 37 °C were used to benchmark the peak position precision using CCSD. Establishing arbitrary common peak lists for all $^{1}H,^{15}N$ spectra recorded at different temperatures were impractical due to difficulty in tracking the shifting of the cross peaks. All $^{1}H,^{15}N$ spectra of the NIST-Fab and two NUS spectra of the SSS were excluded due to the limited number collected. See **Table 1** in main text for descriptions of experiment type.

Excluded $^{1}H,^{15}N$ spectra	Excluded $^{1}H,^{13}C$ spectra from CCSD† only	Excluded $^{1}H,^{13}C$ Spectra from CCSD and PCA‡
E2-1894-101	D2B-2146-003	E1A-1247-002
D1A-2461-101	D2D-2146-005	E1A-1247-004
E2B-2461-108*	D2E-2146-006	E1A-1247-005
E2-3655-101	D2B-6211-405	D2A-1894-102
E2-3655-103*	D2B-6211-406	E1A-1894-103
E2-3676-103*	E1A-6211-408	D2C-1894-104
E2-3676-107*	D2B-6211-409	E1A-1894-105
E2A-4233-117	D2D-6211-410	E1A-1894-106
E2A-4233-123	D2E-6211-411	D3B-2461-107
E2A-4233-142	D3B-6211-412	D2A-3676-102
E2A-4233-148	D2B-6272-005	E1-3676-104
E2B-4533-003	D2D-6272-008	D3A-3676-105
E2-6211-401	D2E-6272-009	E1A-3676-106
E2N-6324-002	D2D-6272-010	E1A-4233-180
E2A-6324-011	D3B-6272-014	D2B-6211-403
E2A-6324-012	D2B-6272-017	E1B-6324-016
E2A-6324-013	D2D-6272-019	D2B-7244-015
D1A-7244-014	D3B-6272-021	E1A-8543-003
E2A-8179-309		E1B-8822-024
E2B-8179-310		E1B-8822-025
E2C-8179-311		E1C-8822-049
E2A-8822-020		
E2A-8822-023		
E2A-8822-026		
E2A-8822-027		
E2C-8822-030*		
E2A-8822-043		
E2B-8822-044		
E2C-8822-047		
E2A-8822-050		
E2C-8822-053		
E2C-8822-057*		
E2N-8822-071		

*$^{1}H,^{15}N$ spectral maps of NIST-Fab
†CCSD = Combined Chemical Shift Deviation
‡PCA = Principal Component Analysis

Table S11. Average ^{1}H,^{15}N chemical shift values for arbitrary peak list from D1A/E2 gHSQC experiments at 37 °C. A 2D ^{1}H, ^{15}N gHSQC with all peaks plotted is given in **Figure S1**. All values are referenced to the methyl resonance of 4,4-dimethyl-4-silapentane-1-sulfonic acid (DSS), which was determined by spiking DSS into a NIST-Fab sample and recording a gHSQC spectrum at 900 MHz. All other spectra were then aligned to peak #68 in bold, whose position was determined to be the same at all temperatures. See Materials and Methods in main text for more details.

Peak	D1A/E2 ^{15}N ppm)	D1A/E2 ^{1}H (ppm)	Peak	D1A/E2 ^{15}N ppm)	D1A/E2 ^{1}H (ppm)	Peak	D1A/E2 ^{15}N (ppm)	D1A/E2 ^{1}H (ppm)
1	101.233	7.814	67	120.097	7.537	133	118.489	8.763
2	105.149	8.923	**68**	**118.978**	**7.546**	134	119.893	8.650
3	107.930	9.086	69	118.764	6.084	135	119.996	8.892
4	108.891	9.096	70	121.571	7.647	136	119.815	8.978
5	110.773	9.135	71	N/A		137	121.808	9.045
6	109.710	10.461	72	120.887	7.743	138	120.906	8.502
7	111.847	9.736	73	121.818	7.753	139	120.782	8.462
8	111.653	9.637	74	123.598	7.793	140	N/A	
9	112.045	8.957	75	124.558	7.769	141	123.042	8.546
10	N/A		76	125.081	7.973	142	123.878	8.776
11	109.991	8.852	77	125.390	7.901	143	125.486	8.789
12	106.763	8.721	78	123.297	7.928	144	129.486	8.567
13	108.604	8.633	79	125.566	7.998	145	130.643	8.444
14	111.552	8.516	80	125.349	8.057	146	N/A	
15	111.214	8.448	81	125.074	8.134	147	N/A	
16	111.379	8.368	82	125.956	8.182	148	130.886	9.163
17	111.311	8.188	83	127.394	8.098	149	N/A	
18	110.077	8.348	84	128.247	8.214	150	129.193	8.846
19	109.599	8.243	85	126.809	8.350	151	129.392	8.914
20	109.692	8.137	86	128.459	8.418	152	129.086	9.011
21	109.755	7.994	87	126.646	8.459	153	128.180	8.819
22	110.632	7.757	88	124.634	8.222	154	127.284	8.850
23	109.054	7.906	89	124.648	8.506	155	126.583	8.884
24	107.613	7.963	90	125.233	8.330	156	N/A	
25	105.592	7.859	91	122.255	8.363	157	123.870	9.124
26	106.997	7.646	92	122.208	8.445	158	123.035	9.104
27	107.613	7.547	93	121.409	8.276	159	122.280	9.285
28	108.777	7.684	94	121.553	8.082	160	123.535	9.293
29	109.503	7.508	95	121.169	8.118	161	124.928	9.319
30	110.900	7.426	96	121.602	7.861	162	125.144	9.224
31	N/A		97	119.680	7.897	163	126.397	9.328
32	109.812	7.232	98	120.425	8.216	164	127.362	9.236
33	109.607	7.135	99	119.641	8.539	165	127.463	9.352

34	106.215	7.154	100	118.690	8.525	166	130.142	9.643
35	108.478	6.978	101	118.071	8.317	167	131.210	9.606
36	106.127	6.500	102	118.158	8.009	168	131.160	9.909
37	104.963	6.158	103	117.883	7.799	169	130.192	10.281
38	110.169	6.406	104	117.681	7.683	170	131.784	10.752
39	109.838	6.621	105	116.673	7.594	171	128.884	10.126
40	110.596	6.658	106	116.839	7.465	172	127.794	10.166
41	110.904	6.766	107	115.903	7.758	173	125.565	10.465
42	112.066	6.940	108	114.746	7.596	174	127.704	9.779
43	112.758	6.910	109	114.373	7.420	175	126.810	9.888
44	112.980	6.840	110	114.016	7.368	176	125.661	9.889
45	112.349	6.837	111	112.836	7.382	177	125.231	9.760
46	112.966	7.299	112	112.983	7.855	178	124.912	9.693
47	112.395	6.744	113	112.381	7.526	179	125.393	9.522
48	112.901	6.779	114	112.056	7.717	180	127.169	9.470
49	111.988	6.581	115	113.189	8.237	181	122.517	9.496
50	113.316	6.550	116	112.962	8.404	182	122.334	9.402
51	114.783	6.776	117	114.583	8.326	183	121.662	9.375
52	N/A		118	114.736	8.191	184	120.014	9.397
53	114.431	6.918	119	115.255	8.278	185	120.736	9.455
54	114.815	7.022	120	115.374	8.366	186	N/A	
55	114.434	7.240	121	116.920	8.413	187	121.632	9.622
56	116.129	6.982	122	116.813	8.489	188	121.638	9.710
57	117.004	7.2578	123	116.544	8.591	189	119.758	9.623
58	118.952	7.317	124	115.773	8.531	190	119.452	9.768
59	119.293	7.194	125	114.412	8.651	191	118.144	10.104
60	119.134	6.950	126	113.978	8.715	192	116.842	10.043
61	121.014	7.093	127	114.124	8.824	193	115.706	9.509
62	121.751	7.208	128	115.669	9.132	194	116.759	9.256
63	122.158	7.424	129	116.226	9.077	195	N/A	
64	120.702	7.319	130	115.469	8.953	196	116.051	8.196
65	120.864	7.405	131	116.395	8.951	197	116.980	8.168
66	120.481	7.475	132	117.113	9.004	198	117.085	8.068

N/A = not applicable. The peak was removed from the reference peak list due to its absence or lack of resolution in a subset of spectra.

Table S12. Average $^{1}H,^{13}C$ chemical shift values for arbitrary peak list from D2A/D2C gHSQC experiments at 37 °C. A 2D $^{1}H,^{13}C$ gHSQC with all peaks plotted is given in **Figures S2** and **S3**. All values are referenced to the methyl resonance of DSS, which was determined by spiking DSS into a NIST-Fab sample and recording a gHSQC spectrum at 900 MHz. All other spectra were then aligned to peak #29 in bold, whose position was determined to be the same at all temperatures. See Materials and Methods in main text for more details.

Peak	D2A/D2C ^{13}C (ppm)	D2A/D2C ^{1}H (ppm)	Peak	D2A/D2C ^{13}C (ppm)	D2A/D2C ^{1}H (ppm)	Peak	D2A/D2C ^{13}C (ppm)	D2A/D2C ^{1}H (ppm)
1	11.559	0.600	38	18.814	0.443	75	N/A	
2	12.221	0.423	39	19.831	0.382	76	23.556	0.637
3	12.561	0.294	40	20.857	0.346	77	22.320	0.553
4	12.841	0.489	41	21.782	0.133	78	22.221	0.427
5	13.308	0.736	42	23.530	0.289	79	21.600	0.351
6	13.665	0.626	43	23.955	0.150	80	21.470	0.283
7	13.634	0.446	44	24.839	-0.011	81	20.378	0.544
8	15.989	0.911	45	25.805	-0.563	82	20.462	0.595
9	16.320	1.740	46	N/A		83	N/A	
10	16.976	1.788	47	N/A		84	20.581	1.266
11	17.164	1.748	48	25.994	0.194	85	20.832	1.399
12	18.207	2.069	49	26.848	-0.062	86	20.971	1.483
13	18.128	1.505	50	26.852	0.278	87	21.767	1.559
14	16.752	1.348	51	27.242	0.477	88	22.039	1.416
15	18.165	1.357	52	27.507	0.638	89	23.007	1.372
16	17.691	1.281	53	27.361	0.763	90	23.625	1.449
17	18.257	1.165	54	28.432	0.901	91	23.697	1.377
18	20.629	1.757	55	27.571	0.898	92	N/A	
19	N/A		56	N/A		93	23.713	1.318
20	N/A		57	27.230	0.981	94	22.802	1.171
21	19.500	1.321	58	26.226	1.045	95	22.601	1.227
22	19.013	1.295	59	26.007	0.925	96	22.609	1.295
23	N/A		60	26.294	0.845	97	22.305	1.320
24	19.522	1.066	61	26.496	0.655	98	21.208	1.326
25	16.988	0.927	62	26.046	0.557	99	20.603	1.005
26	N/A		63	25.254	0.632	100	N/A	
27	18.188	0.692	64	25.515	0.695	101	N/A	
28	17.358	0.646	65	N/A		102	21.186	0.452
29	**17.494**	**0.513**	66	24.558	0.799	103	21.090	0.520
30	17.364	0.387	67	24.295	0.850	104	N/A	
31	17.348	0.222	68	24.915	0.856	105	21.819	0.735
32	17.048	0.100	69	24.687	0.939	106	21.138	0.766
33	14.821	-0.624	70	24.441	0.897	107	21.854	0.796

34	18.875	-0.355	71	25.336	1.021	108	22.230	1.020
35	20.238	-0.196	72	24.167	1.126	109	22.697	1.044
36	N/A		73	23.760	1.003	110	21.598	0.921
37	20.766	-0.084	74	23.344	0.925			

N/A = not applicable. The peak was removed from the reference peak list due to its absence or lack of resolution in a subset of spectra.